



## Original Research Article

# Electricity generation by *Pseudomonas putida* B6-2 in microbial fuel cells using carboxylates and carbohydrate as substrates



Xiaoyan Qi<sup>a</sup>, Huangwei Cai<sup>b</sup>, Xiaolei Wang<sup>a</sup>, Ruijun Liu<sup>a</sup>, Ting Cai<sup>a</sup>, Sen Wang<sup>a</sup>, Xueying Liu<sup>c</sup>, Xia Wang<sup>a,\*</sup>

<sup>a</sup> State Key Laboratory of Microbial Technology, Shandong University, Qingdao 266237, China

<sup>b</sup> Chemical Engineering Department, Columbia University, New York, NY 10027, United States

<sup>c</sup> Powerchina Renewable Energy Co., Ltd., Beijing, 100101, China

## ARTICLE INFO

## Keywords:

Microbial fuel cell  
*Pseudomonas putida* B6-2  
 Multi-substrate biodegradation  
 Power generation  
 Extracellular electron transfer

## ABSTRACT

Microbial fuel cells (MFCs) employing *Pseudomonas putida* B6-2 (ATCC BAA-2545) as an exoelectrogen have been developed to harness energy from various conventional substrates, such as acetate, lactate, glucose, and fructose. Owing to its metabolic versatility, *P. putida* B6-2 demonstrates adaptable growth rates on diverse, cost-effective carbon sources within MFCs, exhibiting distinct energy production characteristics. Notably, the anode chamber's pH rises with carboxylates' (acetate and lactate) consumption and decreases with carbohydrates' (glucose and fructose) utilization. The MFC utilizing fructose as a substrate achieved the highest power density at 411 mW m<sup>-2</sup>. Initial analysis revealed that *P. putida* B6-2 forms biofilms covered with nanowires, contributing to bioelectricity generation. These microbial nanowires are likely key players in direct extracellular electron transport through physical contact. This study established a robust foundation for producing valuable compounds and bioenergy from common substrates in bioelectrochemical systems (BESs) utilizing *P. putida* as an exoelectrogen.

## 1. Introduction

In the face of increasing global energy shortages and environmental pollution, the imperative shift towards replacing fossil fuels with renewable and environmentally friendly energy sources stand out as a key trend in the pursuit of coordinated economic, social, and environmental development [1]. Among the alternative technologies gaining prominence for environmental bioremediation and energy production, bioelectrochemical systems (BESs) have garnered significant attention in recent years [2]. Microbial fuel cells (MFCs), a subset of BESs, represent promising bioreactors that leverage microorganisms as biocatalysts for energy recovery from diverse pollutants, including heavy metals, azo dyes, and antibiotics [2,3]. The concept of MFCs dates back to 1910 when Potter first introduced the idea, employing platinum electrodes to generate electrical energy from cultures of *Escherichia coli* and *Saccharomyces cerevisiae* [4]. Although initial research saw a decline, MFCs resurged in the 1990s, gaining momentum in wastewater treatment, environmental remediation, and sustainable energy production [2,3,5].

The functionality of MFCs hinges on exoelectrogens, which are microorganisms utilizing electrodes either as electron acceptors or donors to catalyze biological processes [2,3]. Therefore, the pivotal elements influencing MFC performance are exoelectrogens with extracellular electron transfer (EET) as the biocatalytic core [6]. Presently, various model exoelectrogens, including *Geobacter sulfurreducens* and *Shewanella oneidensis*, have been extensively studied for their EET capacity through direct or indirect pathways, contributing to the generation of bioelectricity in MFCs [7–9]. *Pseudomonas putida*, a gram-negative aerobic bacterium, showcases its metabolic versatility by efficiently degrading a broad spectrum of aromatic pollutants [10]. Recognized for its potential as an industrial host for valuable compound production [11], *P. putida* stands out due to its extensive metabolic functions and high tolerance to organic solvents and toxic chemicals, setting it apart from conventional industrial hosts like *E. coli* and yeast [11].

Currently, *P. putida* exhibits significant metabolic versatility, utilizing diverse compounds as carbon sources for growth and reproduction. This adaptability contributes to its survival across varied habitats and

**Abbreviations:** BESs, bioelectrochemical systems; CV, cyclic voltammetry; DNS, 3,5-dinitrosalicylic acid; DPV, differential pulse voltammetry; EET, extracellular electron transfer; LB, Luria broth; MFCs, microbial fuel cells; MSM, minimal salt medium; PTS, phosphotransferase system; SCE, saturated calomel electrode; SWV, square wave voltammetry.

\* Corresponding author.

E-mail address: [ghwx@sdu.edu.cn](mailto:ghwx@sdu.edu.cn) (X. Wang).

<https://doi.org/10.1016/j.engmic.2024.100148>

Received 31 October 2023; Received in revised form 18 March 2024; Accepted 21 March 2024

Available online 26 March 2024

2667-3703/© 2024 The Author(s). Published by Elsevier B.V. on behalf of Shandong University. This is an open access article under the CC BY-NC-ND license (<http://creativecommons.org/licenses/by-nc-nd/4.0/>)

enables adjustment to changing environmental conditions [10,12,13]. Biofilm formation in MFCs plays a crucial role in bacterial adsorption, growth, metabolism, and colonization, generating current signals primarily through electroactive biofilms attached to the anode [14]. *Pseudomonas putida* has demonstrated its capability to assimilate various traditional substrates, including glucose, acetate, and lactate, in MFCs, making it a potential electron donor [12,13]. The metabolic versatility of *P. putida* highlights the significant impact of substrates on biological processes such as cell growth, energy production, and compound synthesis [2,13]. Consequently, the selection of appropriate substrates becomes imperative for the effective operation of MFCs utilizing *P. putida* as an exoelectrogen [13].

Although *P. putida* was first identified as an exoelectrogen in 1984, our understanding of its EET mechanism remains preliminary, primarily focusing on exogenous or endogenous redox mediators and microbial nanowires. Exogenous redox substances, such as thionine and  $[\text{Fe}(\text{CN})_6]^{3-/4-}$ , have been verified to enhance EET in BESs with *P. putida* as the exoelectrogen [15,16]. Efforts to enhance EET in BESs include genetic engineering of the phenazine biosynthetic pathway in *P. putida* by Rosenbaum et al. [17–20]. Furthermore, our previous studies have identified microbial nanowires on the biofilms of MFCs utilizing single or mixed aromatic pollutants as substrates, speculating their involvement in direct EET relying on physical contact [21].

Although several conventional substrates have demonstrated potential in MFCs with *P. putida* as the exoelectrogen, there is a lack of studies on the power output of MFCs with different substrates and their associated EET mechanisms [12,13]. Understanding the power output and EET mechanisms of MFCs with different substrates is crucial for future power generation and compound biosynthesis in BESs utilizing *P. putida* as an exoelectrogen. This study investigated power recovery from two model carbohydrates (glucose and fructose) and two model carboxylates (acetate and lactate) in dual-chamber MFCs with *P. putida* B6-2 (ATCC BAA-2545) as the exoelectrogen, focusing on bioelectricity generation, biodegradation, and EET analysis.

## 2. Material and methods

### 2.1. Chemicals and materials

Sodium acetate, sodium lactate, and  $\text{NH}_4\text{H}_2\text{PO}_4$  were procured from Macklin Biochemical Technology Co. Ltd. (Shanghai, China). 3,5-dinitrosalicylic acid (DNS) reagent was obtained from Solarbio Technology Co., Ltd. (Beijing, China). Glucose, fructose,  $\text{K}_3\text{Fe}(\text{CN})_6$ , and methanol were sourced from Sinopharm Chemical Reagent Co. Ltd. (Shanghai, China). All chemicals were of analytical grade, and solutions were prepared using an ultrapure water purification system (Direct-Q3, Merck, USA). Ni-coated sponges were acquired from Huiruhai Technology Co., Ltd. (Shenzhen, China).

### 2.2. Bacterial strain and growth medium

A pure strain of *P. putida* B6-2 (ATCC BAA-2545) served as the anode inoculant for the MFCs, with a nickel-coated sponge as the anode. Luria broth (LB) medium comprised 10 g L<sup>-1</sup> tryptone, 5 g L<sup>-1</sup> yeast extract, and 10 g L<sup>-1</sup> sodium chloride. Minimal salt medium (MSM) included 5.2 g L<sup>-1</sup>  $\text{K}_2\text{HPO}_4$ , 3.7 g L<sup>-1</sup>  $\text{KH}_2\text{PO}_4$ , 2.0 g L<sup>-1</sup>  $\text{NH}_4\text{Cl}$ , 1.0 g L<sup>-1</sup>  $\text{NaSO}_4$ , 0.2 g L<sup>-1</sup>  $\text{MgSO}_4 \cdot 7\text{H}_2\text{O}$ , and a trace mineral stock solution (1%, v/v). The trace mineral stock solution contained 0.3 g L<sup>-1</sup>  $\text{FeCl}_2 \cdot 4\text{H}_2\text{O}$ , 38 mg L<sup>-1</sup>  $\text{CoCl}_2 \cdot 6\text{H}_2\text{O}$ , 20 mg L<sup>-1</sup>  $\text{MnCl}_2 \cdot 4\text{H}_2\text{O}$ , 14 mg L<sup>-1</sup>  $\text{ZnCl}_2$ , 3.4 mg L<sup>-1</sup>  $\text{CuCl}_2 \cdot 2\text{H}_2\text{O}$ , 12.4 mg L<sup>-1</sup>  $\text{H}_3\text{BO}_3$ , and 40 mg L<sup>-1</sup>  $\text{Na}_2\text{MoO}_4 \cdot 2\text{H}_2\text{O}$ . *Pseudomonas putida* B6-2 was initially cultured in 100 mL of LB medium on a rotary shaker (200 rpm) at 30 °C for 12 h. Subsequently, 15 mL cultures were washed twice with MSM, centrifuged at 8000 rpm (6790 g) for 5 min, and then inoculated into the anode chamber containing 150 mL MSM with 2 g L<sup>-1</sup> of glucose, fructose, lactate, and acetate as carbon resources, respectively.

### 2.3. Construction of MFCs

The dual-chamber H-type MFCs were assembled following a previously reported procedure (Fig. S1) [14]. In brief, the 350 mL anode chamber and the 350 mL cathode chamber were separated by a Nafion® N117 proton exchange membrane (Dupont, USA). The anode utilized a Ni-coated sponge with a 5 cm<sup>2</sup> surface area, while the cathode employed double carbon paper with a 10 cm<sup>2</sup> surface area. Copper wires connected the anode and cathode chambers to a data acquisition device with a constant external resistance of 1000 Ω, monitoring real-time potentials every 5 min. The anolyte comprised 150 mL of MSM containing 2 g L<sup>-1</sup> of glucose, fructose, lactate, and acetate, respectively. Simultaneously, the catholyte for these MFCs consisted of a potassium ferricyanide solution (6.93 g L<sup>-1</sup>  $\text{Na}_2\text{HPO}_4$ , 4.77 g L<sup>-1</sup>  $\text{NaH}_2\text{PO}_4$ , and 16.46 g L<sup>-1</sup>  $\text{K}_3\text{Fe}(\text{CN})_6$ ). Throughout MFC operation, each unit was placed in a 30 °C incubator, utilizing a small magnetic stirrer for continuous culture mixing. This temperature is conducive to the growth and metabolism of *P. putida* B6-2 cells in the anode chamber [10].

### 2.4. Detection of bacterial growth, pH change, and substrate concentration

Regularly collected samples from the anode chamber facilitated measurements of bacterial growth, pH changes, and substrate concentrations. A V5100H visible spectrophotometer (METASH, Shanghai) measured bacterial growth, while a SevenCompact™ S210 pH meter (Avantor®, Switzerland) tracked pH changes. Concentrations of acetate and lactate were monitored at 210 nm using an LC-20AT HPLC system (Shimadzu, Japan) equipped with an SPD-20A ultraviolet detector (Shimadzu, Japan) and a C18 column (150 mm length, 4.6 mm inter-diameter, and 5 mm particle size, Thermo, USA) at 35 °C (Fig. S2). Samples underwent elution with a gradient of mobile phases from 0.2%  $\text{NH}_4\text{H}_2\text{PO}_4$  (A) to methanol (B) at a flow rate of 0.5 mL min<sup>-1</sup>, with a phase ratio of A to B at 95:5. Glucose and fructose concentrations were determined using the DNS colorimetric method (Fig. S3). This involved adding 2 mL of DNS reagent to 0.5 mL of the sample, heating in boiling water for 2 min, and adjusting to 15 mL with ultrapure water. The optical density was then measured at 540 nm using a V5100H visible spectrophotometer (METASH, Shanghai).

### 2.5. Measurement of power density and polarization curve

Power density and polarization curves were determined utilizing a PLZ70UA electronic load (KIKUSUI, Japan) through the galvanostatic method [14]. The MFCs under investigation were connected to the electronic load during a stable power generation period. Subsequently, the impressed current was incrementally increased (0.1 mA 100 s<sup>-1</sup>), and voltage data were collected every 10 s. The test procedure and the applied current range are detailed in Table S1. Power density was calculated as  $P=UI A^{-1}$ , where A represents the anode surface area, and I and U denote the current and recorded output voltage, respectively.

### 2.6. Scanning electron microscopy (SEM) characterization of biofilms

In MFCs with different substrates, mature anodic biofilms of *P. putida* gradually formed around the conclusion of the power generation period (approximately 250 h) and were then extracted for SEM characterization. Initially, these biofilms were immersed in 2.5% (v/v) glutaraldehyde and fixed at 4 °C for 12 h. Subsequently, they underwent three washes with sterile ultrapure water to eliminate residual glutaraldehyde solution. The biofilm samples underwent progressive dehydration using an ethanol concentration gradient (30%, 50%, 70%, 80%, 90%, 95%, 100%, and 100%, v/v) for 20 min each. Following this, the pre-treated biofilm samples underwent critical point drying (EM CPD300, Germany) for SEM imaging. Lastly, the samples were mounted on stubs, gold-coated using a vacuum evaporator (Cressington 108, England), and

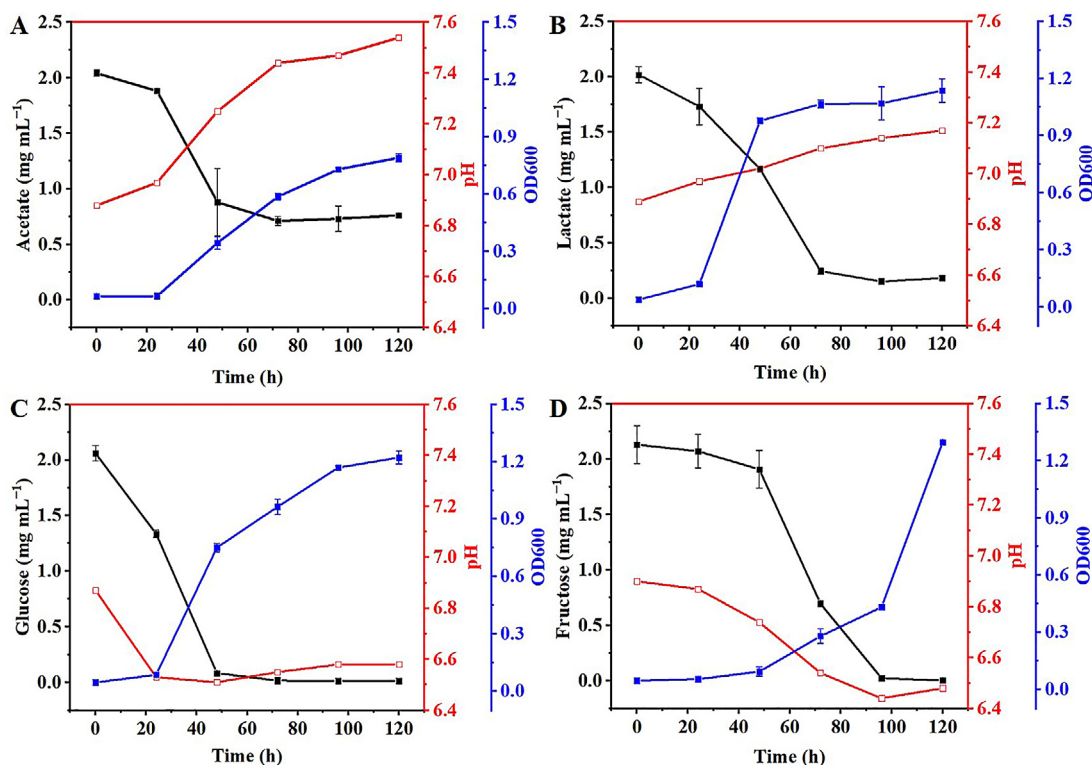


Fig. 1. Bacterial growth, substrate degradation, and pH changes in MFCs with acetate (A), lactate (B), glucose (C), and fructose (D) as substrates, respectively.

imaged using a Quanta 250FEG field-emission scanning electron microscope (FEI, USA).

### 2.7. Electrochemical characterization of cell-free analyte

At the culmination of the power generation, samples were extracted from the anode chamber. These samples were centrifuged at 12,000 rpm for 10 min using Centrifuge 5425 (Eppendorf, Germany) to eliminate suspended biomass from the MFC anolytes. Cyclic voltammetry (CV), square wave voltammetry (SWV), and differential pulse voltammetry (DPV) were performed on cell-free anolytes and controls (MSM containing different substrates) in a three-electrode system using a CHI 760E electrochemical workstation (Chenhua, China). The three-electrode system comprised a glassy carbon electrode as the working electrode, a saturated calomel electrode (SCE) as the reference electrode, and a platinum electrode as the counter electrode.

CV analysis was executed in a potential range of  $-0.6$  V to  $+0.6$  V with a scan rate of  $5$  mV  $s^{-1}$ . SWV analysis was conducted with the following parameters: Initial  $E$   $0.6$  V/ $-0.4$  V, Final  $E$   $-0.4$  V/ $0.6$  V, Incremental  $E$   $2$  mV, Amplitude  $25$  mV, and Frequency  $50$  Hz. DPV analysis was carried out with the following parameters: Initial  $E$   $1.0$  V/ $-0.8$  V, Final  $E$   $-0.8$  V/ $1.0$  V, Incremental  $E$   $4$  mV, Amplitude  $50$  mV, and Pulse width  $50$  mV. CV analysis of anodic biofilms was also performed in  $15$  mL of  $50$  mM phosphate buffer (pH  $7.0$ ) at a scan rate of  $5$  mV  $s^{-1}$ , using the anodic biofilm as the working electrode, and the SCE and platinum electrode as the reference and counter electrode, respectively.

## 3. Results and discussion

### 3.1. Bacterial growth, substrate degradation, and pH changes in MFCs

Individual inoculations of acetate, lactate, glucose, and fructose were introduced into MFCs with *P. putida* B6-2 as the exoelectrogen to observe bacterial growth, substrate degradation, and pH changes (Fig. S4). In

Fig. 1A and B, a brief lag period (approximately 24 h) of growth and rapid substrate degradation were evident in MFCs treated with acetate and lactate, indicating the rapid adaptation of *P. putida* B6-2 to the environment when these compounds served as substrates. Further monitoring revealed limited growth of *P. putida* B6-2 on acetate assimilation compared to lactate, with residual acetate approximately at  $0.66$  mg  $L^{-1}$ . The main inhibitory effects on growth may result from the uncoupling effects of acetate and interference with intracellular anion composition [22,23].

Microbial metabolism involves a series of chemical reactions where microorganisms absorb nutrients to sustain life, proliferate, and degrade substrates [10]. As depicted in Fig. 1, *P. putida* B6-2 exhibited varying degrees of cell growth and organic degradation in the anode chambers with all four substrates as carbon sources, affirming the possibility of metabolic cycling within these MFCs. Fig. S5 illustrates the gradual adsorption of *P. putida* B6-2 onto the anode, forming a mature biofilm. Given that biofilms are typically anaerobic, *P. putida* B6-2 may transfer extracellular electrons to the electrodes, ensuring normal growth, metabolism, and bioenergy production. Consequently, the enhanced growth of *P. putida* B6-2 accelerates microbial biomass in the anode chamber, expediting biofilm formation and potentially shortening the MFC start-up period [24]. Moreover, studies suggest that alternating aerobic and anaerobic conditions enhance EET efficiency and *Pseudomonas* growth on anode biofilms in MFCs [25].

As depicted in Fig. 1C and D, *P. putida* B6-2 efficiently degraded glucose to undetectable levels within 48 h, while this process extended up to 96 h in MFCs utilizing fructose as the sole carbon source. Consequently, the growth rate of *P. putida* B6-2 was notably slower in the presence of fructose compared to glucose alone. Unlike *E. coli* and *Bacillus subtilis*, *P. putida* uptakes glucose through the OprB1 porin in the periplasmic space, rather than utilizing the phosphoenolpyruvate carbohydrate phosphotransferase system (PTS) [26,27]. On the contrary, fructose is the sole carbohydrate known to enter *P. putida* cells via the PTS system [26,27]. Upon cellular uptake, glucose is converted to 6-

phosphogluconate, entering either the pentose phosphate pathway or the Krebs cycle for further utilization [26]. However, fructose, upon uptake by *P. putida* cells, undergoes a series of reactions to transform into glucose-6-phosphate, subsequently utilized through the mentioned glucose catabolic process [26]. The diversity in carbohydrate transport modes and degradation pathways in *P. putida* B6-2 likely contributes to the observed differences in microbial growth and substrate degradation.

In addition, pH changes in the MFCs were measured at 24 h intervals. As illustrated in Fig. 1A and B, the pH of the MFCs with *P. putida* B6-2 as the exoelectrogen continued to increase with the depletion of carboxylates (i.e., acetate, from 6.88 to 7.54; lactate, from 6.89 to 7.17). Conversely, pH decreased with the depletion of carbohydrates (i.e., glucose, from 6.87 to 6.51; fructose, from 6.90 to 6.44) (Fig. 1C and D), caused by various organic acids produced during the metabolism of glucose and fructose [28,29]. Similar results have been reported in previous studies. For example, Thygesen et al. [30] reported an increase in pH from 6.5 to 7.6 during the cultivation period in MFCs with acetate as the substrate; however, when glucose and xylose were used as substrates, the pH decreased from about 7.0 to 4.9 and 5.4, respectively.

Fig. 1 shows that altered pH values in the anode chamber can adversely affect the performance of MFCs, aligning with the fact that *P. putida* B6-2 typically requires a neutral pH for optimal growth. The accumulation of acidic and basic ions results in an excessively acidic and alkaline environment, neither of which is conducive to microbial growth [31]. Additionally, pH fluctuations affect the charged nature of macromolecules in microorganisms and interfere with the normal functions of microbial cells, thereby inhibiting biocatalysis [32]. Taken together, these results indicate that *P. putida* B6-2 can grow and multiply at different rates with a variety of cheap and abundant carbon sources in MFCs, potentially resulting in different power generation characteristics owing to variations in bacterial growth, substrate degradation, and pH changes (Fig. 1).

### 3.2. Power generation efficiency of MFCs with different substrates

To assess the power generation from different substrates, the voltage outputs of the MFCs fed with acetate, lactate, glucose, and fructose were recorded every 5 min. As shown in Fig. 2, all MFCs with *P. putida* B6-2 as the exoelectrogen exhibited a gradual increase in voltage output after connecting an external load of 1000  $\Omega$ . The voltage outputs of the MFCs fed with lactate and glucose reached a plateau after a 24 h start-up period. In contrast, the start-up period was extended to 75 and 48 h for MFCs fed with acetate and fructose substrates, respectively (Fig. 2). This phenomenon may be attributed to the limited microbial growth and slow degradation of acetate and fructose (Fig. 1). Except for the MFC with acetate as the substrate, all the other MFCs demonstrated good power generation performance, with a typical power generation cycle consisting of a sharp start-up phase and a stationary discharge phase lasting approximately 200 h (Fig. 2). The maximum voltages for acetate, lactate, glucose, and fructose were 228, 281, 284, and 436 mV, respectively. Additionally, the voltage outputs of the MFCs with different substrates decreased significantly after 150 h of operation, possibly due to the depletion of carbon sources in these MFCs (Fig. 2). Therefore, the addition of fresh glucose to the anodic chamber of the MFCs led to a significant restoration of the output voltage (Fig. S6).

To further evaluate the power generation characteristics of the MFCs, their power densities and polarization curves were measured using the galvanostatic method. As depicted in Fig. 3, the open-circuit voltages of MFCs with acetate, lactate, glucose, and fructose as substrates were 0.757, 0.805, 0.792, and 0.770 V, respectively. Although the open-circuit voltages of the MFCs with different substrates were similar, the power density of the MFC with fructose as a substrate was 411  $\text{mW m}^{-2}$  (Fig. 3D), which surpassed that of the other MFCs with acetate, lactate, and glucose as substrates, exhibiting power densities of 126, 320, and 317  $\text{mW m}^{-2}$ , respectively (Fig. 3A–C). These variations could be attributed to the distinct pH changes and EET modes during MFC oper-

ation, as well as the metabolic diversity of *P. putida* B6-2 on different substrates [33].

### 3.3. Anodic biofilm analysis of MFCs with different substrates

Microbial EET, a crucial rate-limiting step in MFCs, involves exoelectrogens oxidizing organic or inorganic substances, releasing electrons that are then transferred to extracellular receptors [34,35]. It can be broadly classified into two types: indirect EET via redox mediators and direct EET via physical contact or microbial nanowires [34,35]. Despite considerable interest in EET, it remains a mystery and has been extensively studied mainly in *Shewanella* and *Geobacter* [36,37]. The EET mechanism of *P. putida* has not been thoroughly investigated to date, even though it was identified as a novel exoelectrogen in 1984 [38].

To elucidate the EET mechanism of *P. putida* B6-2, the morphologies of biofilms in MFCs fed with different substrates were characterized using SEM. As depicted in Fig. 4, SEM characterization revealed numerous *P. putida* B6-2 cells adhering to the surface of the anode (nickel-coated sponges) to form a biofilm. This biofilm formation may be facilitated by the continuous open three-dimensional macroporous structure of the nickel-coated sponge, providing a high specific surface area, good biocompatibility, and excellent conductivity conducive to biofilm formation and substrate and electron transfer [14]. MFCs primarily rely on electroactive biofilms for electron delivery through microbial nanowires and/or redox mediators [39,40].

Upon further magnification, the biofilms showed that *P. putida* B6-2 cells produced numerous microbial nanowires, intertwining to form a network structure in the MFCs (Fig. 5). The morphology and structure of these nanowires resemble those formed by *G. sulfurreducens* and *Pseudomonas aeruginosa* [41,42], potentially contributing to the transfer of electrons from *P. putida* B6-2 cells to the anode. Notably, the application of *P. putida* in BESs has been achieved in previous studies with the assistance of exogenous or endogenous redox mediators; therefore, it is often considered as a possible non-native exoelectrogen [15–20]. Our previous study up to 2022 demonstrated that *P. putida* can form nanowire-covered biofilms and generate bioelectricity without the presence of an exogenous redox mediator [21].

Figs. 4 and 5 illustrate that *P. putida* B6-2 formed nanowire-covered biofilms and generated bioelectricity in MFCs with different substrates. These microbial nanowires likely play a pivotal role in direct EET, dependent on physical contact [43], potentially transporting electrons from *P. putida* B6-2 to a distant electrode as an electron acceptor to generate bioelectricity (Fig. S7). To further validate this conclusion, mature biofilms formed in MFCs with different substrates during the stable electrogenesis phase were replaced with new anode materials. As shown in Fig. 6, these MFCs almost lost their electrogenic ability, further suggesting that these physical contact-dependent nanowires likely account for the EET capacity of *P. putida* B6-2. However, the conductivity and molecular biological basis of the nanowires require further exploration in future studies.

### 3.4. Electrochemical analysis of MFCs with different substrates

For indirect EET, various exoelectrogens can generate low molecular weight redox mediators as electron carriers, including flavin derivatives and quinones, enabling electrons to shuttle between the exoelectrogens and the electrode [44–46]. Recent studies have identified phenazine compounds, such as pyocyanin and phenazine-1-carboxamide, produced by *P. aeruginosa*, as driving EET from the bacterium to the electrode [47]. Additionally, the engineering of the phenazine biosynthesis pathway in *P. putida* has been explored to enhance the performance of BESs [17–19]. Various electrochemical analytical methods, such as CV, SWV, and DPV, have successfully been employed to detect and identify various redox mediators in MFCs [44–46].

To investigate whether *P. putida* B6-2 produces redox mediators for EET in MFCs fed with multiple substrates, cell-free anolytes and an-

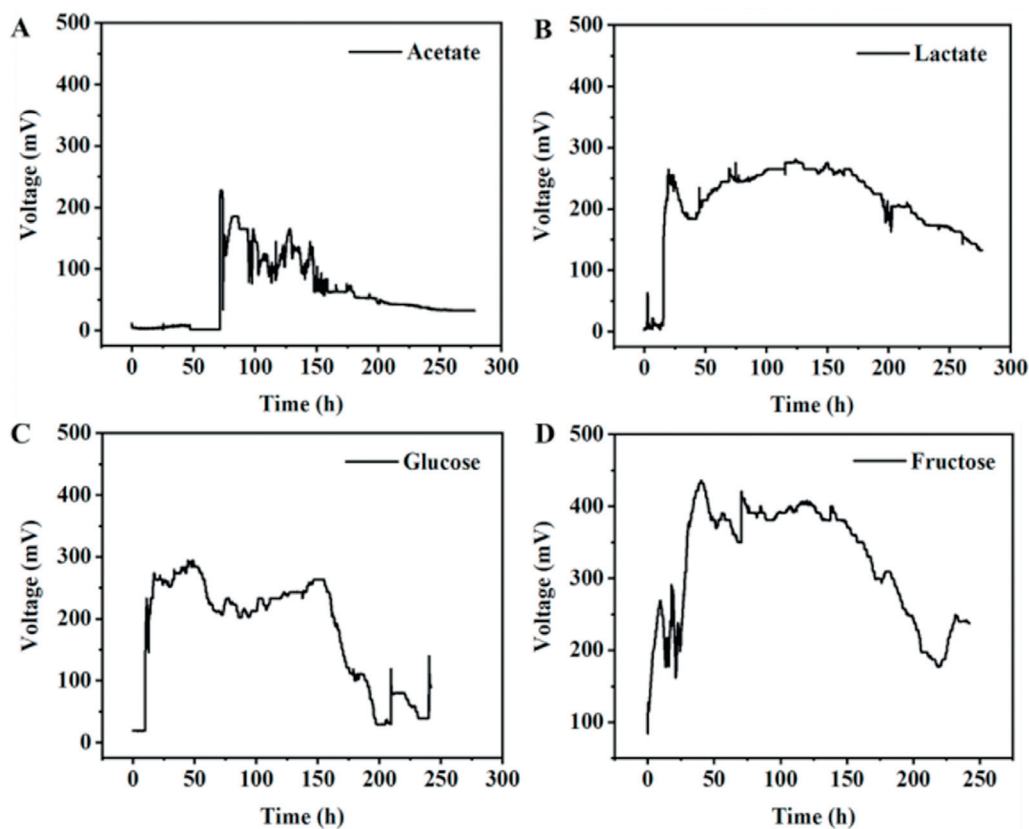


Fig. 2. Voltage output of MFCs with acetate (A), lactate (B), glucose (C), and fructose (D) as substrates, respectively.

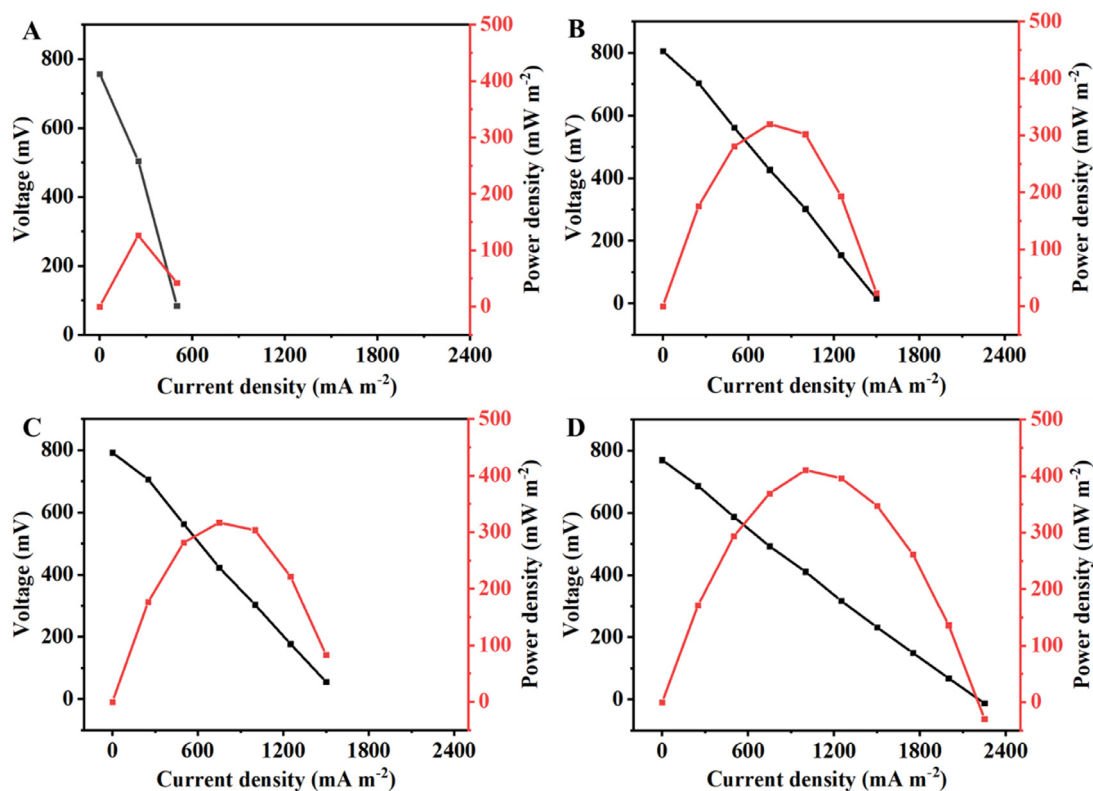


Fig. 3. Power density and polarization curve of MFCs with acetate (A), lactate (B), glucose (C), and fructose (D) as substrates, respectively.

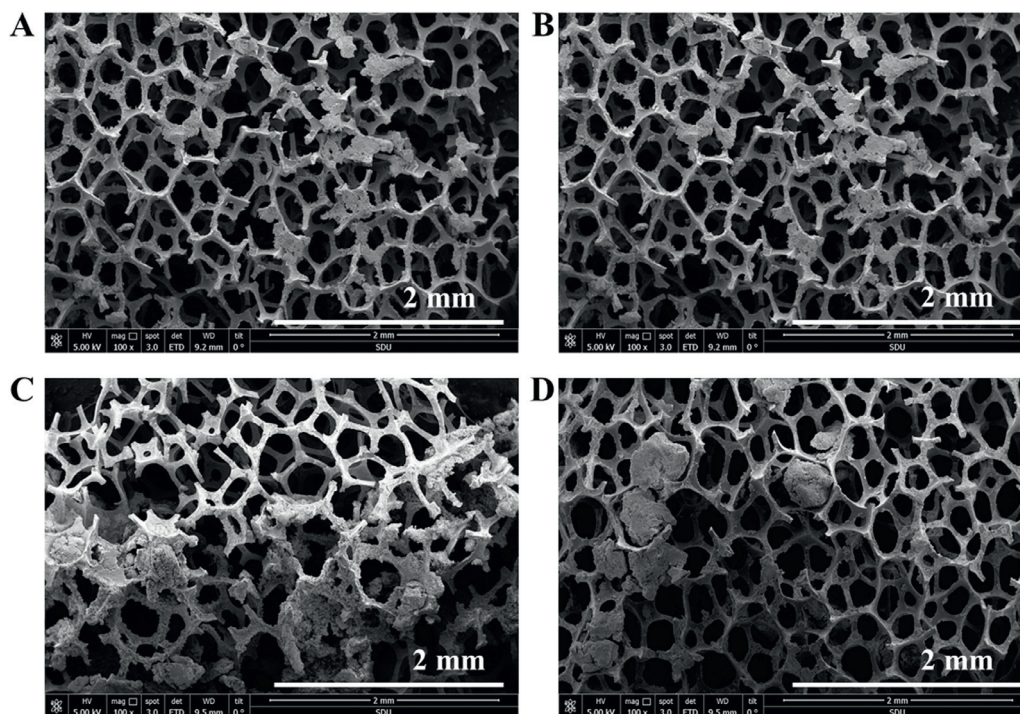


Fig. 4. Morphological analysis of biofilms in MFCs with acetate (A), lactate (B), glucose (C), and fructose (D) as substrates (100 $\times$ ), respectively.

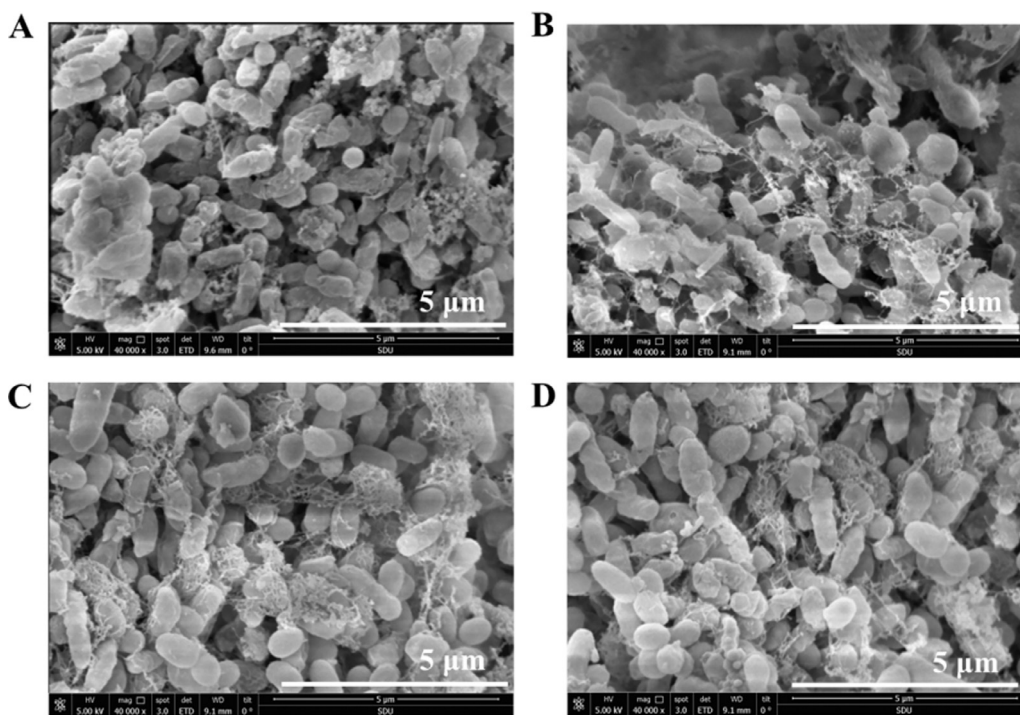


Fig. 5. Morphological analysis of biofilms in MFCs with acetate (A), lactate (B), glucose (C), and fructose (D) as substrates (40,000 $\times$ ), respectively.

odic biofilms were analyzed using electrochemical methods. According to the CV plots, no apparent redox peaks were observed in the cell-free analytes (Fig. 7A–D) and biofilms (Fig. S8) of the MFCs with acetate, lactate, glucose, and fructose as substrates, respectively. This observation suggests that *P. putida* B6-2 did not release or release trace concentrations of redox mediators to enhance the electrochemical activity of the MFCs.

Given that SWV and DPV analyses offer higher sensitivity than CV analysis [48], we utilized SWV and DPV to further characterize redox mediators in cell-free analytes. As depicted in Fig. S9, no significant oxidation or reduction peaks were observed in the SWV analysis. However, in the DPV plots, weak oxidation peaks were noted at approximately +0.2 and +0.8 V compared to the control (Fig. 7E and F), indicating the potential presence of extremely trace amounts of redox mediators.

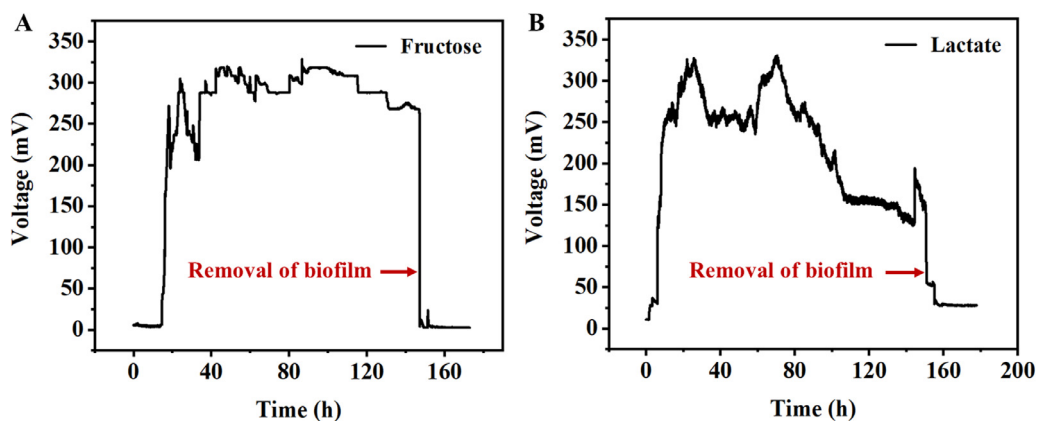


Fig. 6. Voltage output changes after the biofilms were replaced with new anode materials in MFCs with fructose (A) and lactate (B) as substrates, respectively.

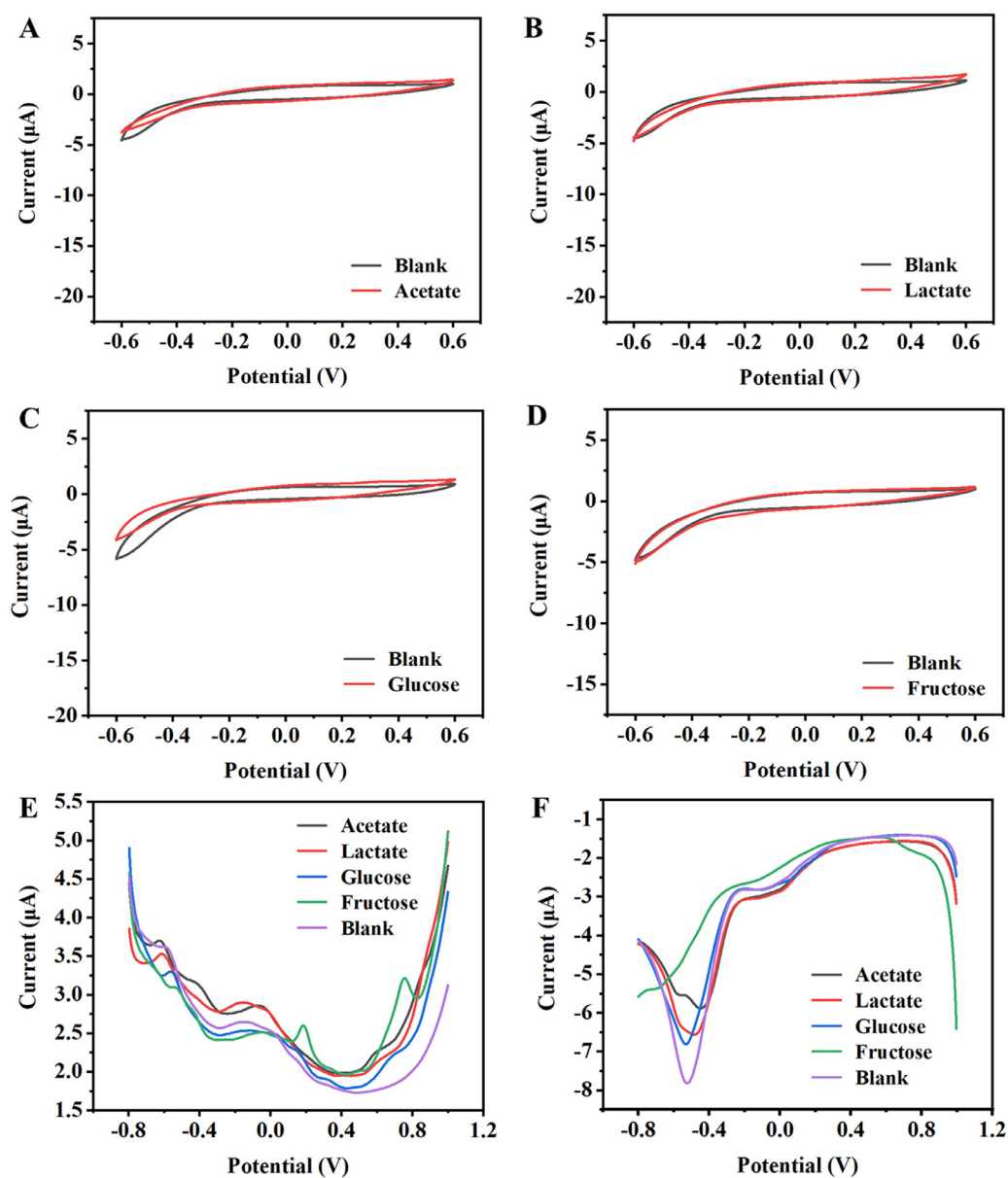


Fig. 7. CV analysis of the cell-free analytes in MFCs with acetate (A), lactate (B), glucose (C), and fructose (D) as substrates, respectively. DPV analysis of the cell-free analytes in MFCs under positive scanning (E) and negative scanning (F).

## 4. Conclusion

Dual-chamber MFCs utilizing *P. putida* B6-2 as the exoelectrogen were successfully established, employing carboxylates (acetate and lactate) and carbohydrates (glucose and fructose) as substrates. The metabolic versatility of *P. putida* B6-2 facilitates effective energy extraction from economical and abundant carbon sources in MFCs. Distinct responses of *P. putida* B6-2 to various substrates resulted in divergent power generation characteristics, encompassing bacterial growth, substrate degradation, pH alterations, and power output features in the MFCs. Initial EET analysis suggested that *P. putida* B6-2 forms nanowire-covered biofilms, contributing to bioelectricity generation. These microbial nanowires likely play crucial roles in the direct EET of *P. putida* B6-2, relying on physical contact. This investigation establishes a groundwork for delving into the mechanisms of direct EET in *P. putida* B6-2, fostering the potential for producing valuable chemicals and bioenergy from conventional substrates in BESSs utilizing *P. putida* as the exoelectrogen.

## Data Availability Statement

All data generated or analyzed during this study are included in this published article (and its Supplementary Materials files).

## Declaration of Competing Interest

The authors declare that they have no known competing financial interests or personal relationships that could have appeared to influence the work reported in this paper.

## CRedit Authorship Contribution Statement

**Xiaoyan Qi:** Writing – original draft, Validation, Investigation, Formal analysis, Data curation. **Huangwei Cai:** Software, Writing – review & editing. **Xiaolei Wang:** Methodology, Investigation, Formal analysis. **Ruijun Liu:** Investigation, Formal analysis. **Ting Cai:** Investigation, Formal analysis. **Sen Wang:** Visualization. **Xueying Liu:** Writing – review & editing. **Xia Wang:** Writing – review & editing, Supervision, Resources, Funding acquisition, Conceptualization.

## Acknowledgements

This work was supported by grants from National Natural Science Foundation of China (32070097 and 91951202), National Key Research and Development Program of China (2019YFA0904800).

## Supplementary Materials

Supplementary material associated with this article can be found, in the online version, at [doi:10.1016/j.engmic.2024.100148](https://doi.org/10.1016/j.engmic.2024.100148).

## References

- N.M. Dowell, P.S. Fennell, N. Shah, et al., The role of CO<sub>2</sub> capture and utilization in mitigating climate change, *Nat. Clim. Change* 7 (2017) 243–249.
- M.A. Abdulwahhab, S.T. Najim, M.A. Abdulwahhab, Microbial fuel cell review: thermodynamic and influencing factors, exoelectrogenic bacteria, anode and cathode configuration, *J. Chem. Technol. Biot. 98* (2023) 1559–1583.
- A.J. Slate, K.A. Whitehead, D.A.C. Brownson, et al., Microbial fuel cells: an overview of current technology, *Renew. Sust. Energ. Rev.* 3 (2010) 899–919.
- M.C. Potter, A.D. Waller, Electrochemical effects accompanying the decomposition of organic compounds, *Proc. Roy. Soc. Lond.* 84 (1911) 260–276.
- H. Wang, J. Park, Z.J. Ren, Practical energy harvesting for microbial fuel cells: a review, *Environ. Sci. Technol.* 49 (2015) 3267–3277.
- D.F. Liu, W.W. Li, Potential-dependent extracellular electron transfer pathways of exoelectrogens, *Curr. Opin. Chem. Biol.* 59 (2020) 140–146.
- S. Ishii, K. Watanabe, S. Yabuki, et al., Comparison of electrode reduction activities of *Geobacter sulfurreducens* and an enriched consortium in an air-cathode microbial fuel cell, *Appl. Environ. Microbiol.* 74 (2008) 7348–7355.
- J.C. Biffinger, J. Pietron, O. Bretschger, et al., The influence of acidity on microbial fuel cells containing *Shewanella oneidensis*, *Biosens. Bioelectron.* 24 (2009) 900–905.
- B. Lai, P.V. Bernhardt, J.O. Krömer, Cytochrome c reductase is a key enzyme involved in the extracellular electron transfer pathway towards transition metal complexes in *Pseudomonas putida*, *ChemSusChem* 13 (2020) 5308–5317.
- W. Wang, Q. Li, L. Zhang, et al., Genetic mapping of highly versatile and solvent-tolerant *Pseudomonas putida* B6-2 (ATCC BAA-2545) as a 'superstar' for mineralization of PAHs and dioxin-like compounds, *Environ. Microbiol.* 23 (2021) 4309–4325.
- A. Loeschcke, S. Thies, *Pseudomonas putida*—a versatile host for the production of natural products, *Appl. Microbiol. Biotechnol.* 99 (2015) 6197–6214.
- M. Rahimnejad, N. Mokhtarian, G. Najafpour, et al., Effective parameters on performance of microbial fuel cell, *Int. Conf. Environ. Comput. Sci.* (2009) 28–30.
- L. Moreno, M. Nemati, B. Predicala, Biokinetic evaluation of fatty acids degradation in microbial fuel cell type bioreactors, *Bioprocess Biosyst. Eng.* 38 (2015) 25–38.
- X. Zhang, H. Wang, T. Xia, et al., Characterization of a new electrochemically active bacterium phylogenetically related to *Alicyclobacillus hesperidum* and its electrochemical performance in microbial fuel cell, *Biosens. Bioelectron.* 175 (2021) 112865.
- S.D. Roller, H.P. Bennetto, G.M. Delaney, et al., Electron-transfer coupling in microbial fuel cells: 1. Comparison of redox-mediator reduction rates and respiratory rates of bacteria, *J. Chem. Technol. Biotechnol.* 34 (1984) 3–12.
- B. Lai, P.V. Bernhardt, J.O. Krömer, Cytochrome c reductase is a key enzyme involved in the extracellular electron transfer pathway towards transition metal complexes in *Pseudomonas putida*, *ChemSusChem* 13 (2020) 5308–5317.
- S. Schmitz, S. Nies, N. Wierckx, et al., Engineering mediator-based electroactivity in the obligate aerobic bacterium *Pseudomonas putida* KT2440, *Front. Microbiol.* 6 (2015) 284.
- T.D. Askitosari, S.T. Boto, L.M. Blank, et al., Boosting heterologous phenazine production in *Pseudomonas putida* KT2440 through the exploration of the natural sequence space, *Front. Microbiol.* 10 (2019) 1990.
- T.D. Askitosari, C. Berger, T. Tiso, et al., Coupling an electroactive *Pseudomonas putida* KT2440 with bioelectrochemical rhamnolipid production, *Microorganisms* 8 (2020) 2–15.
- A. Chukwubulkem, C. Berger, A. Mady, et al., Role of phenazine-enzyme physiology for current generation in a bioelectrochemical system, *Microb. Biotechnol.* 14 (2021) 1613–1626.
- X. Qi, H. Wang, X. Gao, et al., Efficient power recovery from aromatic compounds by a novel electroactive bacterium *Pseudomonas putida* B6-2 in microbial fuel cells, *J. Environ. Chem. Eng.* 10 (2022) 108536.
- S. Pinhal, D. Poppers, J. Geiselmann, et al., Acetate metabolism and the inhibition of bacterial growth by acetate, *J. Bacteriol.* 201 (2019) 147–166.
- M. Basan, S. Hui, H. Okano, et al., Overflow metabolism in *Escherichia coli* results from efficient proteome allocation, *Nature* 528 (2015) 99–104.
- N. Li, R. Kakarla, B. Min, et al., Effect of influential factors on microbial growth and the correlation between current generation and biomass in an air cathode microbial fuel cell, *Int. J. Hydrogen. Energ.* 41 (2017) 20606–20614.
- A. Zani, E.J.R. Almeida, J.P.R. Furlan, et al., Electrochemical skills of *Pseudomonas aeruginosa* species that produce pyocyanin or pyoverdine for glycerol oxidation in a microbial fuel cell, *Chemosphere* 335 (2023) 139073.
- F. Rojo, Carbon catabolite repression in *Pseudomonas*: optimizing metabolic versatility and interactions with the environment, *FEMS Microbiol. Rev.* 20 (2010) 658–684.
- T.D. Castillo, J.L. Ramos, J.J. Rodriguez-Herva, et al., Convergent peripheral pathways catalyze initial glucose catabolism in *Pseudomonas putida*: genomic and flux analysis, *J. Bacteriol.* 189 (2007) 5142–5152.
- C. Ling, G.L. Peabody, D. Salvachua, et al., Muonic acid production from glucose and xylose in *Pseudomonas putida* via evolution and metabolic engineering, *Nat. Commun.* 13 (2022) 4925.
- S. Yu, B. Lai, M.R. Plan, et al., Improved performance of *Pseudomonas putida* in a bioelectrochemical system through overexpression of periplasmic glucose dehydrogenase, *Biotechnol. Bioeng.* 115 (2018) 145–155.
- A. Thygesen, F.W. Poulsen, B. Min, et al., The effect of different substrates and humic acid on power generation in microbial fuel cell operation, *Bioresour. Technol.* 100 (2009) 1186–1191.
- T. Ouyang, X. Hu, X. Shi, et al., Mathematical modeling and performance evaluation of a cathodic bi-population microfluidic microbial fuel cell, *Energ. Convers. Manage.* 267 (2022) 115900.
- X. Zhang, Li X, X. Zhao, et al., Factors affecting the efficiency of a bioelectrochemical system: a review, *RSC Adv.* 34 (2019) 19748–19761.
- A. Weimer, M. Kohlstedt, D.C. Volke, et al., Industrial biotechnology of *Pseudomonas putida*: advances and prospects, *Appl. Microbiol. Biotechnol.* 104 (2020) 7745–7766.
- L. Tao, H. Wang, M. Xie, et al., Improving mediated electron transport in anodic bioelectrocatalysis, *Chem. Commun.* 51 (2015) 12170–12173.
- H. Wang, X. Qi, L. Zhang, et al., Efficient bioelectricity generation and carbazole biodegradation using an electrochemically active bacterium *Sphingobium yanoikuyae* XLDN2-5, *Chemosphere* 307 (2022) 135986.
- G. Reguera, K.D. McCarthy, T. Mehta, et al., Extracellular electron transfer via microbial nanowires, *Nature* 435 (2005) 1098–1101.
- E. Marsili, D.B. Baron, I.D. Shikhare, et al., *Shewanella* secretes flavins that mediate extracellular electron transfer, *Proc. Natl. Acad. Sci. U. S. A.* 105 (2008) 3968–3973.
- S.D. Roller, H.P. Bennetto, G.M. Delaney, et al., Electron-transfer coupling in microbial fuel cells: 1. Comparison of redox-mediator reduction rates and respiratory rates of bacteria, *J. Chem. Technol. Biotechnol.* 34 (1984) 3–12.
- M.J. González-Pabón, E. Cortón, F. Figueredo, Sorting the main bottlenecks to use paper-based microbial fuel cells as convenient and practical analytical devices for environmental toxicity testing, *Chemosphere* 265 (2021) 129101.
- S. Goel, From waste to watts in micro-devices: review on development of membraned and membraneless microfluidic microbial fuel cell, *Appl. Mater. Today* 11 (2018) 270–279.



- [41] D.R. Lovley, J. Yao, Intrinsically conductive microbial nanowires for “green” electronics with novel functions, *Trends Biotechnol.* 39 (2021) 940–952.
- [42] X. Liu, S. Wang, A. Xu, et al., Biological synthesis of high-conductive pili in aerobic bacterium *Pseudomonas aeruginosa*, *Appl. Microbiol. Biot.* 103 (2019) 1535–1544.
- [43] J.C. Biffinger, J. Pietron, R. Ray, et al., A biofilm enhanced miniature microbial fuel cell using *Shewanella oneidensis* DSP10 and oxygen reduction cathodes, *Biosens. Bioelectron.* 22 (2007) 1672–1679.
- [44] B. Huang, S. Gao, Z. Xu, et al., The functional mechanisms and application of electron shuttles in extracellular electron transfer, *Curr. Microbiol.* 75 (2018) 99–106.
- [45] K. Watanabe, M. Manefield, M. Lee, et al., Electron shuttles in biotechnology, *Opin. Biotechnol.* 20 (2009) 633–641.
- [46] T.J. Cameron, J.D. Coates, Review: direct and indirect electrical stimulation of microbial metabolism, *Environ. Sci. Technol.* 42 (2008) 3921–3931.
- [47] X.Y. Yong, D.Y. Shi, Y.L. Chen, et al., Enhancement of bioelectricity generation by manipulation of the electron shuttles synthesis pathway in microbial fuel cells, *Bioreour. Technol.* 152 (2014) 220–224.
- [48] N. Meddings, J.R. Owen, N. Garcia-Araez, A simple, fast and accurate in-situ method to measure the rate of transport of redox species through membranes for lithium batteries, *J. Power Sources* 364 (2017) 148–155.